Nuclear Inst. and Methods in Physics Research, A 911 (2018) 138–141

Contents lists available at ScienceDirect

Nuclear Inst. and Methods in Physics Research, A

journal homepage: www.elsevier.com/locate/nima

Responses of PWO, $LaBr_3$:Ce, and LYSO:Ce scintillators to single-electron hits of 5–40 MeV at KU-FEL

Yusuke Uozumi [a,*], Yuji Yamaguchi [a], Motoharu Fujii [a], Heishun Zen [b], Toshiteru Kii [b], Hideaki Ohgaki [b], Zviadi Tsamalaidze [c], Petr Evtoukhovitch [c]

[a] Kyushu University, Motooka, Nishi-ku, Fukuoka 819-0395, Japan
[b] Institute of Advanced Energy, Kyoto University, Gokasho, Uji, Kyoto 611-0011, Japan
[c] Joint Institute for Nuclear Research, JINR, Joliot-Curie Str.6, Dubna, Russia

ARTICLE INFO

Keywords:
Scintillator
Electron response
Linearity
Pulse shape
Decay time
Single-electron beam

ABSTRACT

The electron responses of PWO, $LaBr_3$:Ce, and LYSO:Ce crystal scintillators have been investigated at the Kyoto University Free Electron Laser (KU-FEL) facility, which provides electron beams satisfying a single-electron hit condition. The linearities and scintillation decay times were measured at electron energies between 5 and 40 MeV. The distributions of pulse height were compared with those from Monte Carlo simulations to deduce the deposit energies. All the scintillators are found to show good linearity, and their decay times are roughly constant over the measured energy range.

1. Introduction

The background of high-energy electrons and photons can occasionally cause interference during nuclear-reaction experiments at a spallation-neutron-source facility. Because crystalline scintillators are frequently used to detect energetic ions, their electron responses (pulse shape and linearity of scintillation light yield) are used to analyze pulse shapes with the aim of filtering out background noise. To this end, it is necessary to know the response characteristics over a wide energy range. To date, many studies have been conducted into the electron responses of certain scintillation crystals. Most of these studies were limited to relatively low energies, below 1 MeV [1–9], because scintillators show remarkable non-proportionality. Only a few studies have been conducted at energies above 1 MeV. Prototype calorimeters were examined [10,11] at very high energies of 0.2–1 GeV for photon-detection purposes in the range of gigaelectronvolts. However, little attention has been given to responses at energies of several tens of megaelectronvolts.

In the present study, we measure electron responses at energies of several tens of megaelectronvolts, a region that has not been studied before. At these energies, the nonlinearity is considered to be weak and the scintillation pulse shapes are generally independent of the bombarding energy. To investigate these points, we use three crystal scintillators: lead tungstate ($PbWO_4$, abbreviated to PWO), cerium-doped lanthanum bromide ($LaBr_3$:Ce), and cerium-doped lutetium–yttrium orthosilicate (LYSO:Ce). PWO crystals are useful for high-energy experiments because of their relatively short decay times (6 and 30 ns) and high density (8.3 g/cm^3). $LaBr_3$:Ce is known to have a short decay time (<25 ns) and a very large photon yield (>60,000 photons/MeV). LYSO:Ce scintillators have decay times of around 40 ns and large photon yields (>35,000 photons/MeV). The purpose of this work is to measure the scintillation decay times and scintillation light yields at electron energies from 5 to roughly 40 MeV.

2. Experiment and analysis

The experiments were carried out at the electron accelerator facility of the Kyoto University Free Electron Laser (KU-FEL) [12]. The facility is shown schematically in plan view in Fig. 1. Electrons with an energy of 8.4 MeV were generated by the thermionic radio-frequency (RF) gun driven by a 10-MW klystron. The electrons were then injected into the traveling-wave-type accelerating tube driven by a 20-MW klystron, where they were accelerated further to 40 MeV. To realize single-electron hits at the detector position (point C), the beam intensity was weakened by turning off the triplet quadrupole *magnets upstream of the undulator and reducing the electron beam current generated by the RF gun by decreasing its thermionic cathode temperature*. Collimators were placed at the entrance and exit of bending-magnet B3 to produce a low-intensity monoenergetic electron beam. The beam was directed to point C and introduced into the scintillator detector in the atmosphere through a 20-μm-thick titanium foil and a slit in the form of a lead block containing a hole 5 mm in diameter and 50 mm in length. This arrangement of equipment around the detector is shown in Fig. 2. The beam intensity

* Corresponding author.
E-mail address: uozumi@kyushu-u.ac.jp (Y. Uozumi).

https://doi.org/10.1016/j.nima.2018.10.040
Received 20 June 2018; Received in revised form 5 October 2018; Accepted 6 October 2018
Available online 12 October 2018

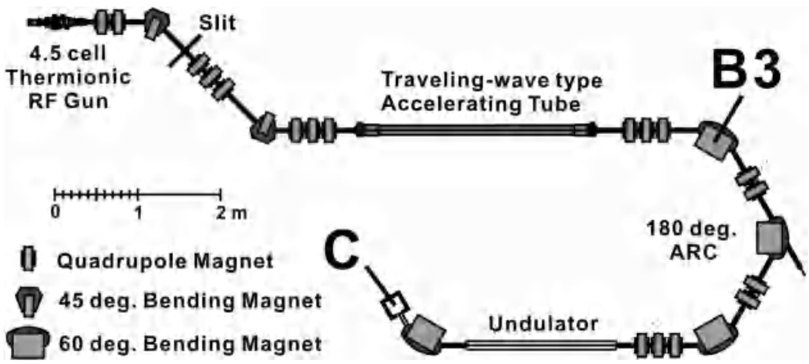

Fig. 1. Plan view of Kyoto University Free Electron Laser (KU-FEL) experimental hall and accelerator.

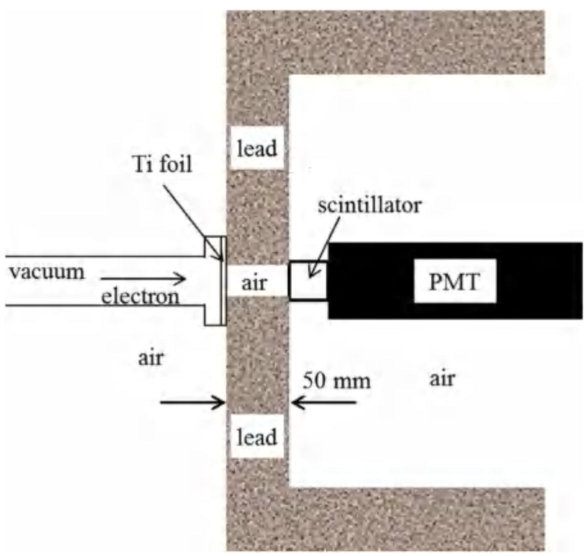

Fig. 2. Geometry around detector for simulation.

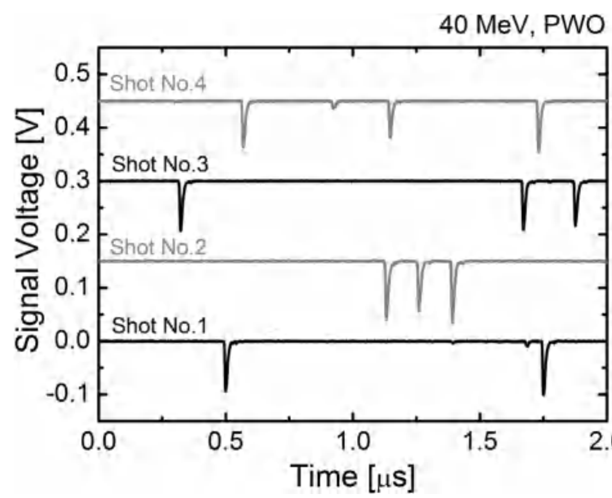

Fig. 3. Single-electron pulses in four shots measured by the PWO scintillator. The electron energy is 40 MeV.

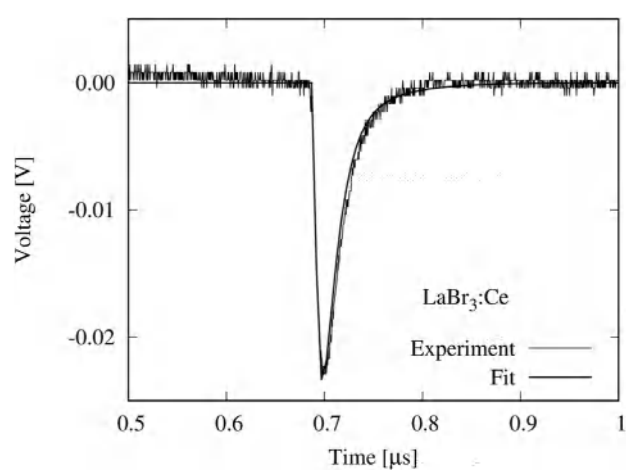

Fig. 4. Scintillation pulse shape of $LaBr_3$:Ce for 40-MeV electron bombardment.

was a few electrons per shot, as shown in Fig. 3, which shows single-electron pulses of 40 MeV observed by the PWO scintillator. Six electron-beam energies, ranging from 5.0 to 40 MeV, were provided for the experiments. The electron beam energy was controlled by the accelerating gradient in the traveling-wave-type accelerating tube shown in Fig. 1. For the 5.0-MeV condition in particular, the electron beam was decelerated from 8.4 MeV to 5.0 MeV in the tube by injecting the electron beam in the deceleration phase. The beam-energy errors were estimated to be less than 1% and were due mainly to *hysteresis of the* electromagnets.

We measured the electron responses of the three scintillator crystals at room temperature. The PWO crystal was a rectangular solid with dimensions of 20 × 20 × 50 mm. The LYSO:Ce was a cylinder 30 mm in length and 30 mm in diameter. The $LaBr_3$:Ce scintillator was a cylinder 38 mm in length and 38 mm in diameter. Each scintillator was coupled directly to a photomultiplier tube (PMT) (R329-02; Hamamatsu Photonics, Japan). The PMT signals were fed into an oscilloscope (DS-5554; Iwatsu, Japan) where the pulse shapes were recorded.

The scintillation pulse shapes were analyzed off-line to obtain the pulse-height distributions and the decay times of the scintillations. The pulse shape $J(t)$ is well expressed [13] as a function of time t by

$$J(t) = -S\left\{\exp\left(-\frac{t-t_p}{\tau_D}\right) - \exp\left(-\frac{t-t_p}{\tau_R}\right)\right\}, \quad (1)$$

where τ_D and τ_R are the decay and rise times, respectively, S is the pulse strength, and t_p is the peak time.

3. Results and discussion

Typical scintillation pulse shapes of $LaBr_3$:Ce and LYSO:Ce observed with 40-MeV electrons are shown in Figs. 4 and 5, respectively. The thin lines are the experimental observations and the thick lines are the results of fitting Eq. (1). For both $LaBr_3$:Ce and LYSO:Ce, the calculations reproduce the experimental pulse shapes well. The resultant values of τ_D for $LaBr_3$:Ce are plotted in Fig. 6 against the deposit energy. The method

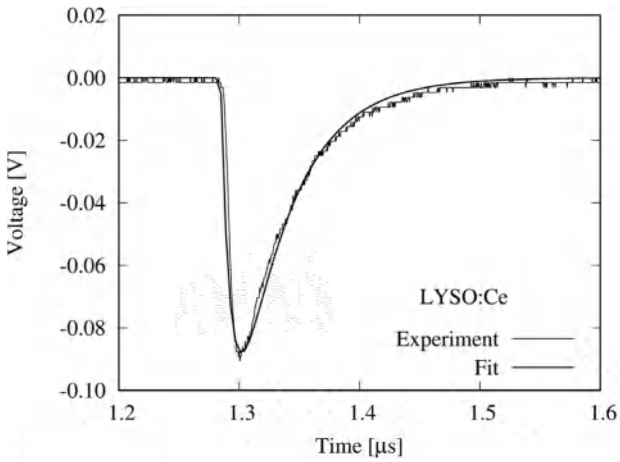

Fig. 5. As Fig. 3 but for LYSO:Ce.

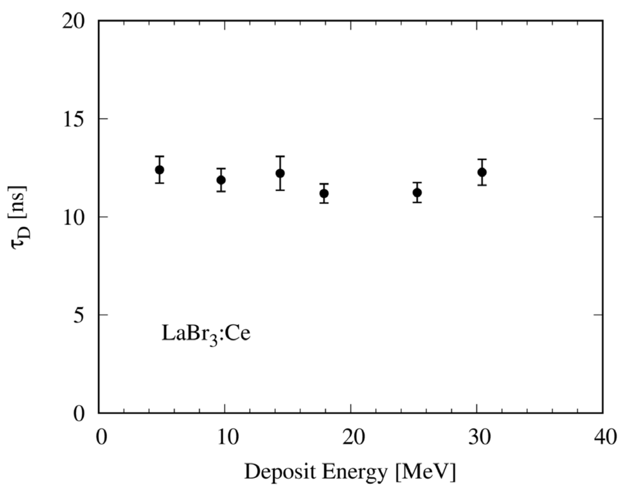

Fig. 6. Decay time of $LaBr_3$:Ce.

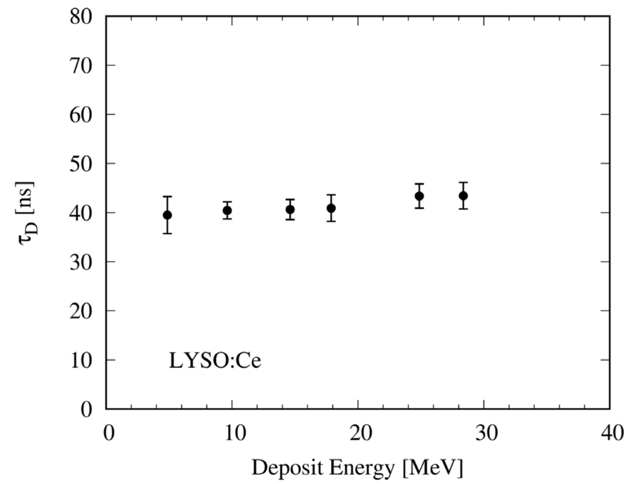

Fig. 7. As Fig. 5 but for LYSO:Ce.

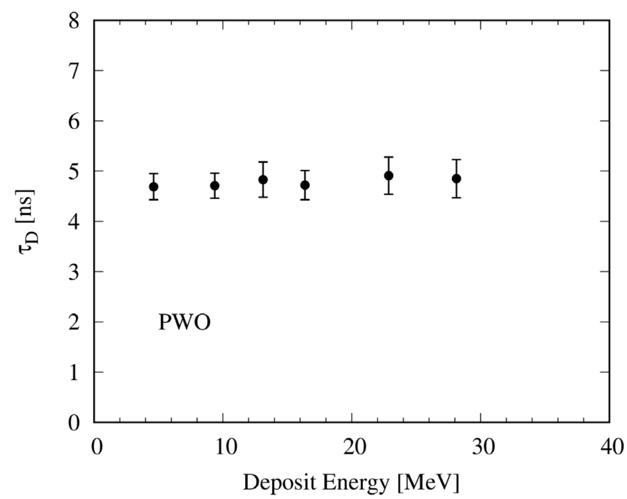

Fig. 8. As Fig. 5 but for PWO.

for determining the deposit energy is described below. The error bars are standard deviations. The values of τ_D are almost constant over the measured energy range. The corresponding energy dependences of τ_D for LYSO:Ce and PWO are shown in Figs. 7 and 8, respectively. The pulse shapes of these scintillators were found to be constant in the present energy range.

The pulse-height distribution of the $LaBr_3$:Ce scintillator for 5-MeV electron bombardment is shown in Fig. 8. The points are the experimental observations and the solid line is the simulation result obtained using the particle transport code PHITS [14,15], which allows full simulation of the measurements of Fig. 2 (i.e., the crystal dimension, the slit in front of the detector, the air between the detector and the accelerator, and the titanium foil as the exit window of the accelerator). In the simulation, the deposit energy distributions to $LaBr_3$:Ce scintillator were calculated first, and then the spectrum was broadened by considering the detector energy resolution. The deposit energies of the experimental observations were normalized by the simulation result. Fig. 10 is the same as Fig. 9 but for an incident electron energy of 40 MeV. For both bombarding energies, the spectral shapes are reproduced well by the simulation. The full energy peak is formed at a beam energy of 5 MeV. In contrast, the spectral peak is at 30.4 MeV for 40-MeV incidence because of the escape of electrons or photons from the volume of the $LaBr_3$:Ce scintillator. The scintillation linearity was investigated using the following procedure. Firstly, a value of the pulse height (voltage) was sampled from the spectrum. Here, we decided to take the peak value of the spectrum.

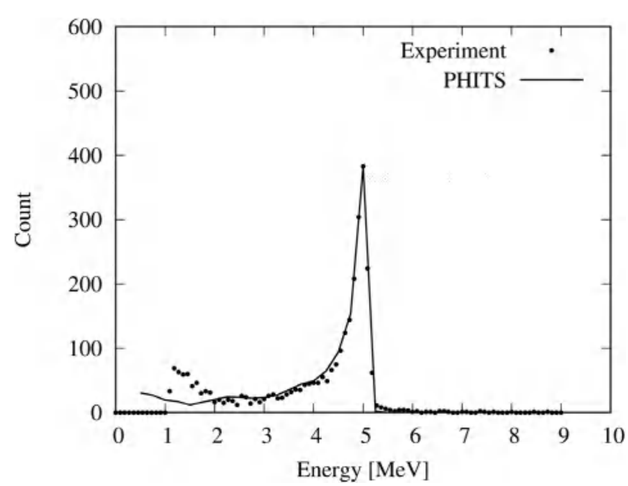

Fig. 9. Pulse-height distribution of $LaBr_3$:Ce scintillator for 5-MeV electron bombardment.

Secondly, the corresponding energy value was determined by fitting the simulated energy spectrum to the experimental pulse-height spectrum. Lastly, we plotted the relationship between pulse height and deposit

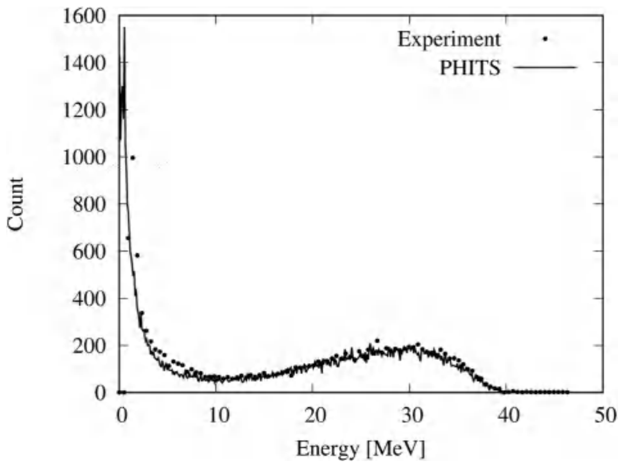

Fig. 10. As Fig. 9 but for electron bombardment of 40 MeV.

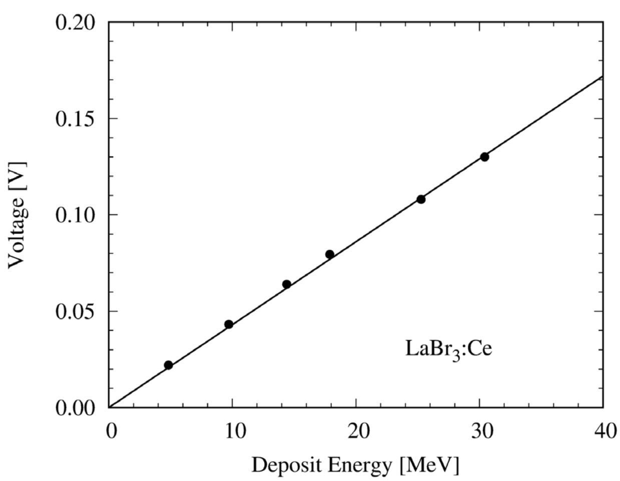

Fig. 11. Linearity of $LaBr_3$ scintillator light output.

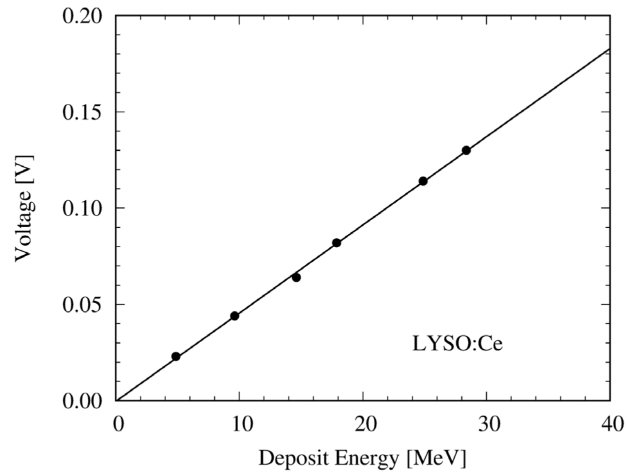

Fig. 12. As Fig. 11 but for LYSO:Ce scintillator.

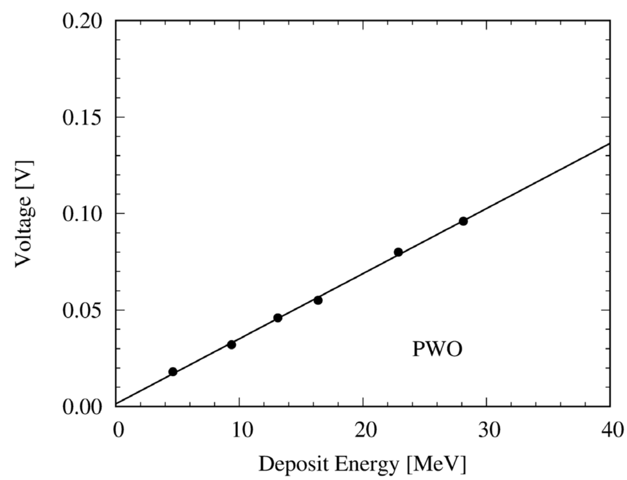

Fig. 13. As Fig. 11 but for PWO scintillator.

energy as Figs. 11–13 for LaBr3:Ce, LYSO:Ce, and PWO, respectively. In this procedure, any possible error is the energy value only, which stems from the fitting uncertainty. The errors were estimated to be 0.7% at most and are smaller than the symbols in the figures. As expected, these scintillators exhibit little nonlinearity in the measured energy range. This result is consistent with the fact that the observed distributions of pulse height and the calculated distributions of deposit energy have almost the same shapes.

4. Conclusion

The electron responses of PWO, $LaBr_3$:Ce, and LYSO:Ce crystal scintillators were measured in terms of their linearities and scintillation decay times at electron energies of 5–40 MeV at KU-FEL, where a single-electron beam is available. The observed pulse-height distributions were reproduced well by Monte Carlo simulation by taking electron scattering into consideration. Each scintillator showed good linearity, and the decay times of the scintillators were roughly constant in the measured energy range.

Acknowledgment

This work was supported by the Joint Usage/Research Program on Zero-Emission Energy Research of the Institute of Advanced Energy, Kyoto University, Japan (ZE29B-32).

References

[1] J.D. Valentine, B.D. Rooney, Nucl. Instrm. Meth. A 353 (1994) 37.
[2] B.D. Rooney, J.D. Valentine, IEEE Trans. Nucl. Sci. 4 (3) (1996) 12–71.
[3] W. Mengesha, T.D. Taulbee, B.D. Rooney, J.D. Valentine, IEEE Trans. Nucl. Sci. 45 (3) (1998) 456.
[4] M. Balcerzyk, M. Moszyński, M. Kapusta, D. Wolski, J. Pawelke, C.L. Melcher, IEEE Trans. Nucl. Sci. 47 (4) (2000) 1319.
[5] Y. Uchiyama, et al., IEEE Trans. Nucl. Sci. 48 (3) (2001) 379.
[6] W.-Seng Choong, G. Hull, W.W. Moses, K.M. Vetter, S.A. Payne, N.J. Cherepy, J.D. Valentine, IEEE Trans. Nucl. Sci. 55 (3) (2008) 1073.
[7] M. Moszyński, Rad. Meas. 45 (3–6) (2010) 372.
[8] P.B. Ugorowski, M.J. Harrison, D.S. McGregor, Nucl. Instrum. Meth. A615 (2010) 1–82.
[9] I.V. Khodyuk, J.T.M. de Haas, P. Dorenbos, IEEE Trans. Nucl. Sci. 57 (3) (2010) 1175.
[10] R. Novotny, W. Doring, K. Mengel, V. Metag, C. Pienne, IEEE Trans. Nucl. Sci. 44 (3) (1997) 477.
[11] H. Shimizu, Y. Sakamoto, T. Hashimoto, K. Abe, Y. Asano, T. Kinashi, T. Matsumoto, T. Matsumura, H. Okuno, H.Y. Yoshida, Nucl. Instrum. Meth. A447 (3) (2000) 467.
[12] H. Zen, T. Kii, K. Masuda, H. Ohgaki, T. Yamazaki, Infrared Phys. Technol. 51 (5) (2008) 382.
[13] P.A. Rodnyi, Physical Process in Inorganic Scintillators, CRC Press, Boca Raton, 1997.
[14] L. Sihver, et al., Adv. Space Res. 45 (7) (2010) 892.
[15] T. Sato, et al., J. Nucl. Sci. Tech. 50 (9) (2013) 913.